

Fractional quantum Hall physics with ultracold Rydberg gases in artificial gauge fields

F. Grusdt^{1,2} and M. Fleischhauer¹¹*Department of Physics and Research Center OPTIMAS, University of Kaiserslautern, Germany*²*Graduate School Materials Science in Mainz, 67663 Kaiserslautern, Germany*

(Received 20 July 2012; revised manuscript received 9 April 2013; published 23 April 2013)

We study ultracold Rydberg-dressed Bose gases subject to artificial gauge fields in the fractional quantum Hall (FQH) regime. The characteristics of the Rydberg interaction give rise to interesting many-body ground states different from standard FQH physics in the lowest Landau level. The nonlocal but rapidly decreasing interaction potential favors crystalline ground states for very dilute systems. While a simple Wigner crystal becomes energetically favorable compared to the Laughlin liquid for filling fractions $\nu < 1/12$, a correlated crystal of composite particles emerges already for $\nu \leq 1/6$ with a large energy gap to the simple Wigner crystal. The presence of a new length scale, the Rydberg blockade radius a_B , gives rise to a bubble crystal phase for $\nu \lesssim 1/4$ when the average particle distance becomes less than a_B , which describes the region of saturated, almost constant interaction potential. For larger fillings indications for strongly correlated cluster liquids are found.

DOI: 10.1103/PhysRevA.87.043628

PACS number(s): 67.85.-d, 73.43.Cd, 32.80.Qk, 32.80.Ee

I. INTRODUCTION

In the context of the fractional quantum Hall effect (FQHE) interesting many body ground states exist, some of which carry fractional and non-Abelian braiding statistics [1–5]. This makes them ideal candidates for a topological quantum computer [6,7] and gives access to topological quantum phases [8]. For an experimental study a high degree of control is required and quasi-two-dimensional (quasi-2D) ultracold gases of atoms in artificial magnetic fields have been suggested as potential candidates [9]. Effective magnetic fields are generated either by rotation [10,11], employing light-induced gauge potentials [12–16], or in lattices with complex hopping amplitudes [17,18]. When a weakly interacting superfluid Bose gas is rotated sufficiently fast an ordered vortex-lattice forms [19,20] and the lowest Landau level (LLL) regime can be reached [21]. Although for bosonic atoms there is no integer quantum Hall effect based on the Pauli principle, repulsive interactions can give rise to highly correlated FQH states for fillings $\nu \lesssim 6$ [9] when only the LLL is occupied [22–24]. However, despite the experimental progress strongly correlated phases have not been realized yet. In part this can be attributed to the rather small interaction energies in atomic gases. In the present paper we propose an alternative approach using $1/r^6$ van der Waals (vdW) interactions in Rydberg states. The associated energies can be orders of magnitude larger than those achievable with contact or magnetic dipole-dipole interactions [25] making Rydberg interactions an ideal candidate for the realization of FQH physics. It is also possible to hybridize Rydberg atoms with light in form of so-called Rydberg polaritons [26], which opens the possibility to realize FQH physics with photons. Here artificial gauge fields can be generated either by rotation of a suitable medium [27] or using waveguide lattice structures [28].

In the present paper we theoretically analyze the phase diagram of particles with a Rydberg interaction in the LLL using exact diagonalization (ED) as well as variational methods. Similar to dipolar gases with $1/r^3$ interaction, which have been extensively studied in the past [29–31], we find a transition from Laughlin (LN) liquids [32] to crystalline ground states for very dilute systems, however with an extended filling

region where only composite particles can crystallize at zero temperature. In contrast to dipolar gases the difference in variational energy between composite crystals and simple Wigner crystals is rather large. Additionally, the presence of a new length scale, the so-called Rydberg blockade radius a_B gives rise to a clustering mechanism supporting bubble crystal ground states for fractional fillings $\nu \leq 1/4$. For larger fillings we find in the regime of large blockade radii indications for very interesting cluster liquids.

II. RYDBERG DRESSED ATOMS AND PSEUDOPOTENTIALS IN THE LLL

Recently, there has been a lot of interest in atoms excited to high Rydberg states and there has been considerable experimental progress to make these systems accessible [33–39]. Of particular interest in the present context are atoms excited by far-off resonant laser radiation. In this case, called Rydberg dressing [see Fig. 1(a)], the atoms essentially remain in their ground state but show an effective interaction [40,41] [see Fig. 1(b)]

$$V(r) = \frac{\tilde{C}_6}{a_B^6 + r^6}, \quad a_B = \left(\frac{C_6}{2\hbar\Delta} \right)^{1/6}. \quad (1)$$

For large particle separations r the interaction potential is of vdW type $\sim r^{-6}$, where $\tilde{C}_6 = (\Omega/2\Delta)^4 C_6$ describes the effective interaction strength with C_6 being the bare vdW coefficient, $\Omega \ll |\Delta|$ the Rabi frequency of the laser excitation, and Δ its detuning. Since bare Rydberg interaction energies are typically many orders of magnitude stronger than, e.g., magnetic dipole-dipole interactions, the excitation gap of FQH states can easily reach the energy separation between Landau levels (LLs). Most importantly the interaction potential (1) flattens off below the blockade radius a_B , thereby defining a new characteristic length scale. We note that the same behavior of the interaction potential is found for Rydberg polaritons [42], which makes it possible to apply many of the results obtained here to FQH physics of photons hybridized with Rydberg atoms.

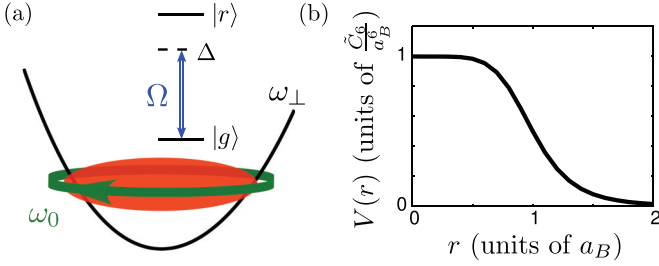


FIG. 1. (Color online) (a) An ultracold Bose gas is dressed with Rydberg excitations $|r\rangle$ by illuminating with a far-off-resonant (detuning Δ) laser beam Ω . Rotating the gas with frequency ω_0 and applying a weak harmonic trap ω_\perp in radial and a tight one in the transverse direction ($\omega_\perp \gg \omega_0$) the quasi-2D FQH regime can be reached. (b) Interaction potential for Rydberg-dressed atoms.

To be specific, we consider in the following a continuous gas of Rydberg atoms for which the effective magnetic field is created by rotation, noting, however, that the results carry over to lattice systems with not too large flux per plaquette [43]. When a Rydberg-dressed Bose gas is set into rotation with angular frequency ω_0 in a radial trap of frequency ω_\perp , the characteristic oscillator length scale is given by $\ell_c = (2m_a\omega_\perp/\hbar)^{-1/2}$ [44], with m_a the atomic mass. The competition of the two length scales ℓ_c and a_B leads to interesting new physics. Already in the mean-field regime where the rotation frequency is well below the deconfinement limit ($\omega_\perp > \omega_0$) there is, e.g., a transition from a vortex lattice to a supersolid phase [45]. Here we are interested in the regime of strong correlations. To this end we consider a Rydberg-dressed Bose gas in the LLL regime for fillings $\nu < 1$, assume a quasi-2D gas, neglect finite-thickness effects, and use $\omega_\perp = \omega_0$. In the latter case ℓ_c is replaced by the magnetic length $\ell_c \rightarrow \ell_B$. For simplicity we consider only even values of $1/\nu$ corresponding to bosonic LN states.

The interaction projected to the LLL is described by Haldane's two-particle pseudopotentials V_m [46], where the integer m denotes the relative angular momentum. In disk geometry the pseudopotentials are given by

$$V_m = \frac{1}{2^{2m+1}m!} \int_0^\infty dr r^{1+2m} V(r) e^{-r^2/4}, \quad (2)$$

where for bosons (fermions) only $m = 0, 2, 4, \dots$ ($m = 1, 3, 5, \dots$) are relevant.

The dominant energy scale is determined by the lowest pseudopotential V_0 , while the higher-order terms typically fall off very fast. For a strict point interaction in the LLL all V_m 's vanish identically except for $m = 0$. Tables I and II list some explicit values of V_0 for Rb. There we assume a fixed magnetic length $\ell_B \approx 1\mu\text{m}$ (corresponding

TABLE I. Realistic blockade radii a_B and energies V_0 for Rb with $\omega_c \approx 2\pi \times 130$ Hz (i.e., $\ell_B \approx 1\mu\text{m}$), $\Delta = 10\Omega = 2\pi \times 1$ GHz as a function of the principle quantum number n .

n	40	50	60	70	80	90	100
a_B (μm)	0.97	1.5	2.0	2.7	3.4	4.3	5.2
$V_0/2\pi$ (kHz)	2.8	5.3	7.9	9.9	11.2	11.8	12.1

TABLE II. Realistic blockade radii a_B and energies V_0 for Rb with $\omega_c \approx 2\pi \times 130\text{Hz}$ (i.e., $\ell_B \approx 1\mu\text{m}$), $n = 46$ as a function of the detuning of the dressing laser Δ . Note that the Rabi frequency Ω was chosen as $\Omega = 0.1\Delta$.

Δ (MHz)	1.0	9.0	80	700	20×10^3
a_B (μm)	3.94	2.73	1.90	1.32	0.76
$V_0/2\pi$ (kHz)	0.0744	0.574	3.75	20.8	240.0

to $\omega_c \approx 2\pi \times 130$ Hz, which is a realistic value [47]) as well as a fixed ratio $\Omega/\Delta = 0.1$. For the $60S_{1/2}$ Rydberg state in Rb, $C_6(n = 60)/2\pi = 0.14$ THz μm^6 and we used the scaling law $C_6(n) \propto n^{11}$ [48]. In Table I $\Delta = 2\pi \times 1$ GHz is constant and the principle quantum number of the Rydberg state n is varied. In Table II, on the other hand, $n = 46$ is fixed and the detuning Δ is varied. Note that by varying Δ it is possible to tune the interaction potential adiabatically.

One recognizes rather large values of V_0 up to hundreds of kHz, which can easily become comparable to or even exceed the typical LL splitting ω_c . Thus, different from all previously discussed interactions in cold gases the characteristic energy scales for Rydberg-Rydberg interactions must be limited by demanding LLL approximation (i.e., $V_0 < \hbar\omega_c$).

Table III lists some explicit values of higher pseudopotentials V_m for the vdW interaction (1). They are also plotted in Fig. 2 together with contour lines of the continuous function $V(m) = V_m$ for $m \in \mathbb{R}$ defined as in (2) above. One recognizes that at given a_B the first V_m are approximately equal until the radial extent $R_m = \sqrt{2m}\ell_B$ of the wave function in the relative coordinate is $\sim a_B$. The subsequent pseudopotentials decrease quickly.

The relevance of the pseudopotentials becomes apparent if one considers the (bosonic analog of the) Laughlin wave function for the ground state of N particles at filling $\nu = 1/n$, with n being an (even) integer. Denoting the coordinate of the j th particle in the 2D plane by the normalized complex variable $z_j = (x_j + iy_j)/\ell_B$ the LN wave function reads [32]

$$\psi_{\nu=1/n}(z_1, \dots, z_N) \sim \prod_{i < j} (z_i - z_j)^n e^{-\frac{1}{4} \sum_k |z_k|^2}. \quad (3)$$

In the absence of interactions and any confinement potential all states are degenerate and have zero energy. When considering the contribution of the interaction Hamiltonian to the energy of the LN states one recognizes that the Jastow factors $\prod_{i < j} (z_i - z_j)^n$ eliminate, furthermore, all contributions from pseudopotentials V_m with $m = 0, 2, \dots, n-2$. As a consequence the energy scale of the ground state at filling $\nu = 1/m$ is set by the largest unscreened pseudopotential, i.e., by V_m .

For this reason, the curve $\sqrt{2m}\ell_B = a_B$ separating the two regions in the contour plot of pseudopotentials in Fig. 2 also separates two parameter regions with qualitatively different physics for a given filling fraction ν ,

$$\sqrt{2/\nu}\ell_B < a_B \quad \text{and} \quad \sqrt{2/\nu}\ell_B > a_B. \quad (4)$$

The first region corresponds to at most one particle per blockade area on average, while the second corresponds to more than one particle in that area.

TABLE III. Leading-order bosonic (m even) pseudopotentials V_m for the potential Eq. (1) discussed in the main text.

a_B/ℓ_B	$V_0 (\tilde{C}_6/\ell_B^6)$	V_2/V_0	V_4/V_0	V_6/V_0	V_8/V_0	V_{10}/V_0	V_{12}/V_0	V_{14}/V_0
0.1	3.015×10^3	1.40×10^{-5}	2.16×10^{-7}	4.30×10^{-8}	1.54×10^{-8}	7.19×10^{-9}	3.91×10^{-9}	2.37×10^{-9}
0.2	1.871×10^2	1.69×10^{-4}	3.48×10^{-6}	6.95×10^{-7}	2.49×10^{-7}	1.16×10^{-7}	6.31×10^{-8}	3.82×10^{-8}
0.3	3.652×10^1	6.93×10^{-4}	1.78×10^{-5}	3.56×10^{-6}	1.27×10^{-6}	5.95×10^{-7}	3.23×10^{-7}	1.96×10^{-7}
1	2.455×10^{-1}	3.43×10^{-2}	2.53×10^{-3}	5.28×10^{-4}	1.89×10^{-4}	8.82×10^{-5}	4.80×10^{-5}	2.91×10^{-5}
2	9.816×10^{-3}	0.223	4.56×10^{-2}	1.24×10^{-2}	4.66×10^{-3}	2.20×10^{-3}	1.20×10^{-3}	7.28×10^{-4}
3	1.172×10^{-3}	0.505	0.203	8.06×10^{-2}	3.55×10^{-2}	1.77×10^{-2}	9.91×10^{-3}	6.04×10^{-3}
4	2.314×10^{-4}	0.740	0.450	0.250	0.137	7.75×10^{-2}	4.63×10^{-2}	2.92×10^{-2}
5	6.279×10^{-5}	0.877	0.680	0.479	0.322	0.212	0.140	9.47×10^{-2}
10	9.996×10^{-7}	0.996	0.987	0.970	0.944	0.908	0.863	0.811

III. GROUND STATE FOR SMALL BLOCKADE RADII

In the following we discuss the ground state of the system in the case of a small blockade radius $a_B < \ell_B \sqrt{2/\nu}$, where its effect can be disregarded.

A. The $\nu = 1/2$ and $\nu = 1/4$ ground states

For $a_B/\ell_B \rightarrow 0$ the first two pseudopotentials diverge,

$$V_0 \approx \frac{3}{8} \frac{\tilde{C}_6}{\ell_B^6} \left(\frac{\ell_B}{a_B} \right)^4, \quad V_2 \approx \frac{1}{2^6} \left(0.571 - \ln \frac{a_B}{\ell_B} \right) \frac{\tilde{C}_6}{\ell_B^6}, \quad (5)$$

while all $V_{m>2}$ converge. Therefore, the $\nu = 1/2, 1/4$ bosonic LN states are exact ground states. To understand the effect of finite (but small) blockade radii we performed ED calculations in spherical geometry for small particle numbers N . Table IV lists overlaps to the Laughlin states for $N = 6$ particles and several a_B . The results remain valid even for larger particle numbers: We obtain overlaps squared of, e.g., 0.992 for $\nu = 1/2$ and $N = 10$ and 0.974 for $\nu = 1/4$ and $N = 7$. Some remarks on the ED simulations are given in the Appendix.

B. Ground states at small fillings

Now we want to address the physics for small fillings, i.e., $\nu < 1/4$, again for $a_B \lesssim \ell_B$. Due to the nonlocal interaction a natural ground-state candidate in this regime is the non-correlated Wigner crystal (NWC) [49] described by the wave

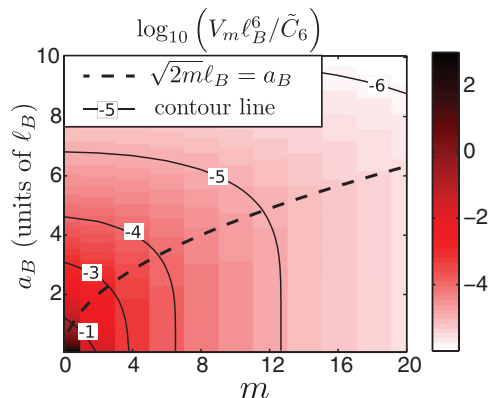


FIG. 2. (Color online) Contour plot of pseudopotentials V_m for the potential (1), where m was treated as continuous parameter for better illustration. Black solid lines denote contours of constant (continuous) pseudopotential.

function

$$\psi_{\text{NWC}}(z) = \mathcal{S} \prod_j e^{-(z_j - R_j)^2 + z_j R_j^* - z_j^* R_j} / 4, \quad (6)$$

where $R_j \in \mathbb{C}$ defines a lattice in the plane of complex coordinates $z_j = (x_j + iy_j)/\ell_B$ and \mathcal{S} stands for complete symmetrization.

1. Variational ground-state energy

To see if the NWC could be a ground state we compare the corresponding variational energy per particle ϵ_{NWC} to that of the LN state. To this end we generalize the expression for ϵ_{NWC} derived in [49] to bosons,

$$\epsilon_{\text{NWC}} = \frac{1}{2} \frac{\tilde{C}_6}{\ell_B^6} \sum_{j \neq 0} \frac{e^{-|R_j|^2/4}}{1 + \frac{1}{2} e^{-|R_j|^2/2}} K(\xi = |R_j|), \quad (7)$$

$$K(\xi) = \int_0^\infty \frac{dr r e^{-r^2/4}}{r^6 + (a_B/\ell_B)^6} \left(I_0 \left(\frac{r\xi}{2} \right) + J_0 \left(\frac{r\xi}{2} \right) \right),$$

where I_0, J_0 denote Bessel functions. The integral can be handled numerically and the lattice sum can easily be performed. Like for electrons [49,50] and dipolar fermions [51], the lattice that minimizes the NWC energy is a hexagonal one, see Fig. 3.

In Fig. 3 the energies of different NWCs and the LN liquid are plotted for small $a_B = 0.2\ell_B$ and even values of $1/\nu$. The energy of the LN liquid was calculated using the standard plasma analogy [32] for $N = 100$ particles for all examined ν using a Metropolis Monte Carlo (MC) algorithm [52]. We find a transition from LN to a NWC for

$$\nu \leq \nu_{\text{NWC}} = \frac{1}{14}, \quad (8)$$

TABLE IV. Overlaps squared of the ground state to the Laughlin states at fillings $\nu = 1/2, 1/4$. They were obtained using ED at $N = 6$ in spherical geometry. We write 0 when our value is below the numerical precision, i.e., $< 10^{-15}$.

a_B/ℓ_B	$\nu = 1/2$	$\nu = 1/4$
6.1	1.690×10^{-09}	0
5.1	4.935×10^{-10}	0
4.1	7.303×10^{-10}	0
3.1	2.594×10^{-03}	0.9026
2.1	0.9940	0.9696
1.1	0.9998	0.9960
0.1	0.999 999 999 978	0.999 88

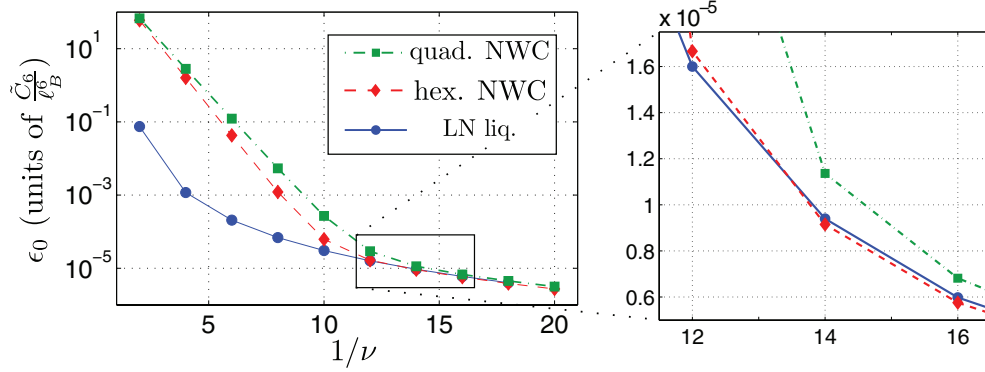


FIG. 3. (Color online) Comparison of the variational energies per particle ϵ_0 (at fillings $\nu = 1/2, 1/4, 1/6, \dots$, corresponding to the bosonic Laughlin states) for the different trial wave functions at $a_B = 0.2\ell_B$ (LN, Laughlin states; NWC, noncorrelated Wigner crystal of bare particles).

although for $\nu = 1/12$ the energy difference is so small that we cannot exclude a transition here. Interestingly, this value of the critical filling is far below the corresponding value of $\nu \approx 1/7$ found for pure Coulomb and dipolar interacting fermions [50,51,53]. Due to the more local nature of the vdW interaction potential, this is not surprising: For pointlike interactions there is no crystallization at all.

2. Stability of Wigner crystal

In an alternative approach we can determine the stability region of a lattice using, e.g., the Lindemann criterion. To this end we calculate the Lindemann parameter $\gamma \equiv \sqrt{\langle \delta \mathbf{u}^2 \rangle} / a$ from the phonon spectrum in harmonic and nearest-neighbor approximation following [54], where a denotes the (hexagonal) lattice constant and $\delta \mathbf{u}$ the atomic displacement from the lattice $\{R_j\}$. The phenomenological criterion states that the crystal melts when γ exceeds a critical value γ_c . In our case $\gamma = 0.57\sqrt{\nu}$ for $a_B < \ell_B$ at zero temperature, and $\gamma_c \approx 0.28$ [51,55]. Thus, the crystal is expected to be stable for

$$\nu < \nu_{\text{Ld}} = \frac{1}{4}, \quad (9)$$

similar to the result found in dipolar systems [30,51]. This value differs significantly from the transition point to a NWC, $\nu_{\text{NWC}} = 1/14$, found above.

3. Gap to collective excitations and spatial correlations

For small system sizes (see Appendix) and small $a_B \lesssim \ell_B$ the exact ground state has relatively large overlap to the LN liquid and the spectrum shows a low-lying exciton branch. On the other hand, the analysis of the previous section suggests that in the thermodynamic limit the true ground state may not be a LN liquid. Thus, to investigate the nature of the ground state in the region of intermediate fillings we calculate the energy gap ΔE of LN states to collective excitations using ED in spherical geometry. More specifically, ΔE is the difference from the ground to first excited state, where the latter can well be described as a density wave and exhibits a roton minimum [56,57]. In Fig. 4 ΔE is plotted for $\nu = 1/6, 1/8$ for finite size systems and extrapolations to the thermodynamic limit are shown. Also shown are the results for $\nu = 1/4$

for comparison, which clearly yield a positive gap in the thermodynamic limit. Although the system sizes which we were able to reach with our ED are not very large, they do allow for an extrapolation to the infinite size limit and indicate negative gaps—i.e., instability—for $\nu = 1/6$ and $\nu = 1/8$.

In Fig. 5 second-order correlations, $g^{(2)}(r) = \langle \hat{\psi}^\dagger(0)\hat{\psi}^\dagger(r)\hat{\psi}(r)\hat{\psi}(0) \rangle$ are shown for $\nu = 1/8$ and $a_B = 0.2\ell_B$. We find strongly enhanced oscillations for $N = 6$ signaling a trend towards long-range order. For $N = 5$ this effect is absent, which can be attributed to a more general finite-size effect: Already for the gaps (Fig. 4) we observe a slightly different behavior for N even/odd and $\nu = 1/6, 1/8$. For $N = 2, 4, 6$, ΔE is smaller than for $N = 3, 5$ and we find the same behavior for the ground-state energy. This is another indication for crystallization, since also for a classical vdW crystal on a sphere the ground-state energy per particle shows these oscillations due to incommensurability.

These numerical findings for small systems support the result of the Lindemann stability analysis, that crystallization occurs below $\nu = 1/4$. That raises the question about the nature of the ground state for fractional fillings in the range $1/4 > \nu \geq 1/14$.

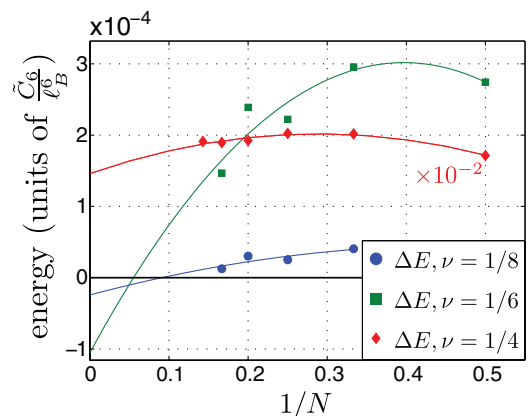


FIG. 4. (Color online) Gap to collective excitations ΔE at $\nu = 1/4, 1/6, 1/8$ and for $a_B = 0.2\ell_B$. Note that for $\nu = 1/4$ energies were scaled down by a factor of 100. ED in spherical geometry was used and finite-size corrections were performed as described in the Appendix. Solid lines, quadratic fits.

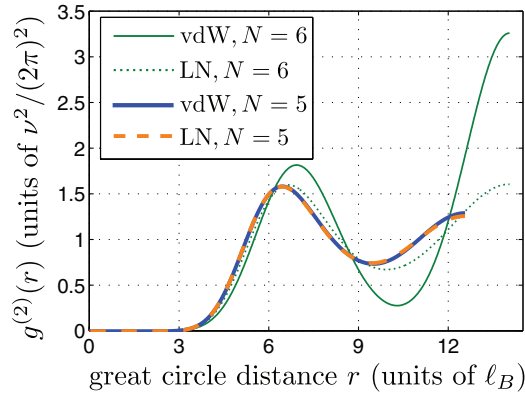


FIG. 5. (Color online) Second-order correlation functions, $g^{(2)}(r)$, of the ground state for van der Waals (vdW) interactions at $a_B = 0.2\ell_B$ and $\nu = 1/8$, compared to those of the corresponding LN liquids for different system size ($N = 6$ thin, $N = 5$ thick). ED in spherical geometry was used.

C. Correlated Wigner crystal of composite particle

Instead of a NWC the ground state in the region $\nu_{\text{Ld}} > \nu \geq \nu_{\text{NWC}}$ could be a crystal of composite particles (CPs) [58], termed *correlated* Wigner crystal (CWC) [59,60]. As for the LN states the first pseudopotentials are screened for CPs and only the effects of the long-range tails of the repulsive interaction potential remain. As the latter should be the same for CPs as for bare particles the stability arguments given above remain valid and a CWC should form already for $\nu < \nu_{\text{Ld}} = 1/4$.

CWC variational wave functions of the form

$$\psi_{\text{CWC}}^{(\mu)}(z) = \mathcal{P}_{\text{LLL}} \prod_{j < k} (z_j - z_k)^\mu \psi_{\text{NWC}}(z)$$

were investigated in [59] using MC simulations based on the plasma analogy, and the critical filling $\nu \approx 1/7$ in electronic, i.e., fermionic systems was correctly predicted. Here \mathcal{P}_{LLL} is a projector to the LLL and $(z_j - z_k)^\mu$ are Jastrow factors describing the formation of μ -composite bosons CB^μ (fermions CF^μ) for μ even (odd). We here performed similar MC simulations and calculated the variational energy of hexagonal CWCs for different μ . From the plasma analogy it can be concluded [59] that the lattice constant a used for the NWC have to be rescaled in the definition of the CWC wave function in order to produce the desired density at filling ν :

$$a \rightarrow a(1 - \mu\nu). \quad (10)$$

In the MC simulations we take into account only direct but no exchange terms but have checked that the first exchange corrections are negligible. Our results are shown in Fig. 6 and we observe that for $\nu \leq 1/6$ CWCs are energetically favorable compared to LN states.

We thus expect crystalline order already for $\nu < \nu_{\text{Ld}} = 1/4$, in agreement with the stability analysis and long before the simple NWC becomes energetically favorable at $\nu = \nu_{\text{NWC}}$. More specifically we expect a CB^4 CWC ground state at $\nu = 1/6$ and $\nu = 1/8$. For $\nu = 1/10$ the CB^4 and CF^5 CWCs are equal in energy within our MC errors and we cannot make a final conclusion about the underlying CPs. Most importantly, the variational energy of the composite crystals is for a larger

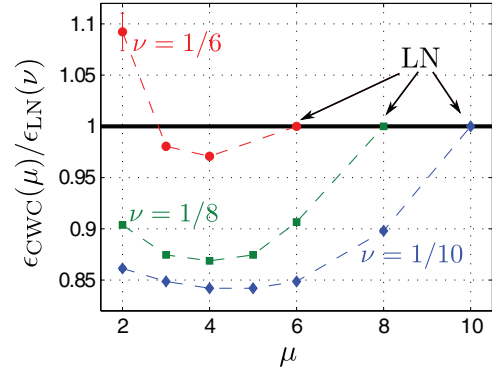


FIG. 6. (Color online) Variational energy per particle of the hexagonal CWC of CP^μ , $\epsilon_{\text{CWC}}(\mu)$, in units of the LN state energy $\epsilon_{\text{LN}}(\nu)$ at filling ν . Results were obtained in Metropolis MC simulations with $N = 91$ particles.

range of fractional fillings substantially below the value of the NWC.

That crystals of CPs are formed for $\nu < 1/4$ is further supported by the ED results for the second-order correlation function plotted in Fig. 5. For larger distances r one recognizes enhanced oscillations of $g^{(2)}(r)$ as compared to those expected for LN liquids. On the other hand, the correlations decay still according to a power law for small r , e.g., $g^{(2)}(r) \sim r^{11}$ for $N = 6$ at $\nu = 1/8$. This is a direct indication that the ground-state physics of these systems is dominated by CP^μ 's with μ between 4 and 6, as predicted above.

IV. EFFECTS OF FINITE BLOCKADE RADIUS

We now discuss the effects of the saturation of the effective vdW interaction potential, Eq. (1), for distances less than the blockade radius a_B . As we show the competition of the magnetic length ℓ_B with the new length a_B will give rise to new physics which has similarities with physics of higher LLs in the solid-state context. Specifically we consider the case where there are more than two particles per blockade area $A_B = \pi a_B^2$, i.e., the regime $a_B \gtrsim \sqrt{2/\nu\ell_B}$.

A. Bubble crystal at small fillings

ED results obtained on spheres suitable for LN states show that for $a_B \lesssim \sqrt{2/\nu\ell_B}$ and $\nu = 1/4$ or $1/2$, the ground state is a ν LN state with vanishing angular momentum $L = 0$. For $a_B \approx \sqrt{4/\nu\ell_B}$ a transition to a $L \neq 0$ state is observed, which after mapping from sphere (radius R) to plane (momentum k), $kR = L$ [61], corresponds to a breaking of translational invariance. Figure 7 shows numerical results for the two-particle correlation $g^{(2)}(r)$ for different ratios of a_B/ℓ_B . For small a_B ($L = 0$ phase) we find LN-like correlations while for large a_B ($L \neq 0$ phase) we find particle bunching at $r = 0$, which indicates clustering. Clustering of k particles can also be seen in the $k + 1$ -st-order density correlations,

$$g^{(k+1)}(z) \equiv \langle (\hat{\Psi}^\dagger(0))^k \hat{\Psi}^\dagger(z) \hat{\Psi}(z) (\hat{\Psi}(0))^k \rangle.$$

For example, for $a_B = 2.9\ell_B$, $k = 2$ particles cluster, resulting in a very small $g^{(3)}(0) \approx 2 \times 10^{-5}(\nu/2\pi)^3$ (for $\nu = 1/2, N = 8$), while $g^{(2)}(0) = 0.9(\nu/2\pi)^2$ is still large.

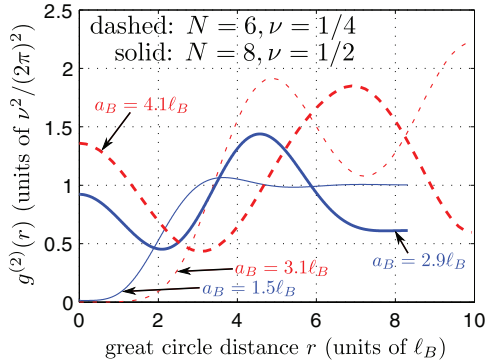


FIG. 7. (Color online) Second-order correlation function for the ground state for increasing values of a_B for $N = 8$, solid line ($N = 6$, dashed line) for $\nu = 1/2$ ($\nu = 1/4$). For large a_B symmetry is broken ($L \neq 0$ thick lines), in contrast to small a_B ($L = 0$ thin lines).

These numerical findings can be explained as follows: For $a_B > \sqrt{4/\nu} \ell_B$ where there are more than two particles per A_B , the long-range contribution to the interaction energy can be reduced by bringing the particles inside A_B together. At the same time there is no energy penalty from interactions inside A_B since the potential (1) is constant for $r \lesssim a_B$. This provides a pairing mechanism. Assuming that all particles within A_B undergo clustering, one expects a transition from $k - 1$ to k particles per cluster at $a_B^{(k)} = \sqrt{2k/\nu} \ell_B$.

By analogy we expect the formation of a NWC consisting of clusters, when the reduced filling of the system with clusters $\nu_{\text{cl}} = \nu/k$ is small. This state is referred to as bubble crystal (BC) and was, e.g., considered for electrons in a weak magnetic field where $\nu > 1$, i.e., beyond the LLL [62]. The present situation is comparable since the effective interaction in a higher LL is “smeared out” around $r = 0$, making it qualitatively similar to our interaction Eq. (1). A BC phase was also predicted for dipolar bosons at filling $\nu = 1/2$ with large finite-thickness effects [63]. To verify that BCs are indeed good ground-state candidates for large blockade radii we calculate the variational energy per particle by generalizing (7). This yields

$$\epsilon_{\text{BC}}(k; \nu) = k \epsilon_{\text{NWC}}(\nu = \nu_{\text{cl}}) + (k - 1) V_0, \quad (11)$$

where the second term describes the binding energy per particle required for the cluster formation. In Fig. 8 the ground-state phase diagram is shown determined by comparing the variational energies of the LN liquid, the NWC, and the BC. Also shown are the transition points between symmetry-conserving ($L = 0$) and symmetry-breaking ($L \neq 0$) states obtained from ED. One recognizes that BC ground states with $k \geq 2$ particles per cluster exist for $\nu \leq 1/4$ and $a_B \gtrsim a_B^{(2)}$.

B. Speculations for large filling: Cluster liquids

For $\nu = 1/2$ the BC is higher in energy than the LN state for all a_B and for sufficiently large $a_B \gtrsim a_B^{(2)}$ the LN state is no longer a good ground-state candidate. Therefore, the nature of the ground state for large a_B and large filling is an open question. In the following we give some speculative arguments about the ground state in this parameter region. In contrast to other regions here only numerical results from ED for up to $N = 10$ particles are available and thus it is difficult to make

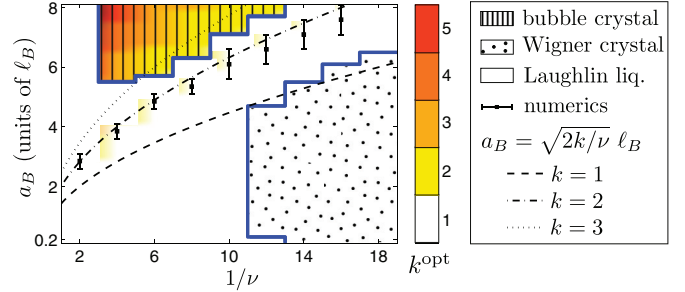


FIG. 8. (Color online) Phase diagram (for $1/\nu \in 2\mathbb{N}$) obtained from the comparison of variational energies of LN state ($N = 100$ using Metropolis MC) and BC. The optimal number k^{opt} of particles per cluster (color code) was used in the BC region. The squares with error bars show the phase transition from LN to a symmetry-breaking state obtained numerically (ED, spherical geometry).

definite statements. Clearly, further studies are needed here. Yet our preliminary studies show that this parameter regime could be a very interesting one.

Besides clustered crystalline states of the type discussed above, many different correlated cluster liquids have been proposed and discussed in the context of the FQHE in higher LLs. Most prominent are the Read-Rezayi (RR) \mathbb{Z}_k parafermion states [64] which have recently been generalized using totally symmetric Jack polynomials [65]. The Haffnian (Hf) [66] is another example not contained in the Jack series. These states are characterized by the number of particles per cluster k (e.g., $k = 2$ for Hf) and the exponent r which determines the short-distance behavior of the correlations $g^{(k+1)}(z) \sim |z|^{2r}$. For Hf $r = 4$ and for all RR states $r = 2$. For filling $\nu = 1$ the Moore-Read Pfaffian (Pf) [3] (the $k = 2$ RR state) was shown to be the ground state for dipolar [31] and contact [24] interactions corresponding to $a_B \ll \ell_B$. We also find a large overlap to the Pf of, e.g., $|\langle \psi(N = 12) | \text{Pf} \rangle|^2 = 0.90$ for $a_B = \ell_B$. Since the potential (1) provides a clustering mechanism also for $\nu < 1$, the cluster liquids are reasonable trial wave functions for our situation as well.

In the following we focus on filling $\nu = 1/2$, where the BC is no ground state. We investigate the three simplest $\nu = 1/2$ cluster liquids, namely the LN state ($k = 1, r = 2$), the Hf ($k = 2, r = 4$), and the $k = 3, r = 6$ Jack polynomial. We refer to the latter as 3-6 BH (Bernevig, Haldane) state. As in the BC case, we expect a transition from $k - 1$ to k particles per cluster at $a_B^{(k)}$. This estimates the transition from LN to Hf to be at $a_B^{(2)} \simeq 2.8 \ell_B$ and from Hf to 3-6 BH at $a_B^{(3)} \simeq 3.5 \ell_B$. In Fig. 9(a) we show the numerically obtained overlaps of the ground state wave functions with the trials. (The 3-6 BH state is obtained from the “Jack generator” [68].) Note that the calculations were done for spheres of the different sizes supporting the respective trial ground states. We find that for every a_B at least one of the overlaps takes a substantial value. This finding must be taken with care, however: It is known that when a trial wave function has a large overlap to the exact ground state for small systems, this does not imply a good description in the thermodynamic limit. The transitions between the different trial states in Fig. 9 are reasonably well described by the above estimates. Coexistence of phases is a finite size effect, at least partly caused by the different system sizes.

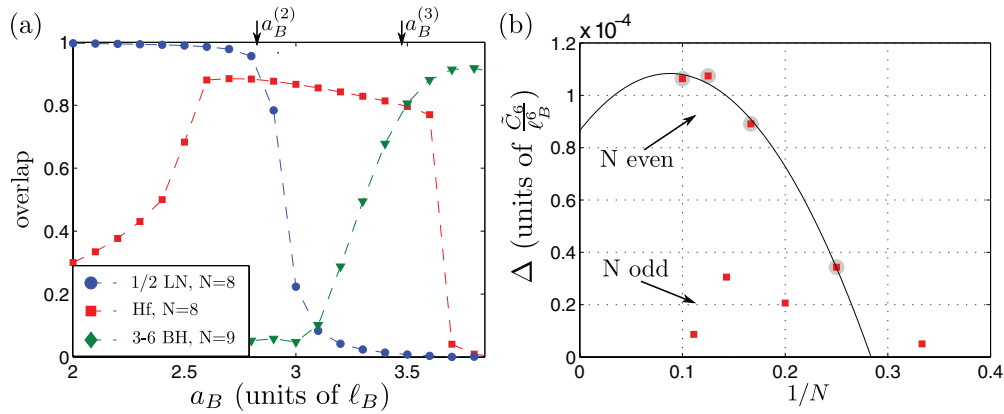


FIG. 9. (Color online) ED results in spherical geometry. (a) Overlap of the numerically determined ground states to the different trial wave functions. (b) Finite size approximation of the gap to collective excitations for the ground state at the system size of the Hf (at $a_B = 3\ell_B$). Finite size corrections were carried out following [67]. The different behavior of Δ for N even/odd is another indication of cluster formation with $k = 2$ particles per cluster.

We close our discussion of cluster liquids by investigating the ground-state excitation gap. In Fig. 9(b) finite size approximations are shown for the Hf state which suggest that it is an incompressible ground state in the thermodynamic limit. This is a surprising result since the Hf is generally believed to describe compressible states. We note that the arguments given by Green [66] that the Hf lies on a phase transition and should be gapless rely on the fact that the effective CB^2 interaction is purely repulsive. It was shown for composite fermions (CFs) that a flattening of the bare $1/r$ potential leads to attractive inter-CF interactions [69]. By analogy we speculate that for our extremely flat potential (1) the inter- CB^2 interactions becomes attractive as well, which will indeed lead to CB^2 pairing [70]. We also note that even our bare potential has a small attractive component in momentum space. Whether or why the pairing symmetry should be d -wave as required for the Hf will be devoted to future work.

We conclude this section by noting that this parameter regime, which may be easier accessible experimentally than the low-filling regimes discussed above, is potentially a very interesting one. In order to make more definite statements further studies are needed, however.

V. SUMMARY

Summarizing, we have shown that Rydberg-dressed Bose gases can give rise to extremely strong interactions and a

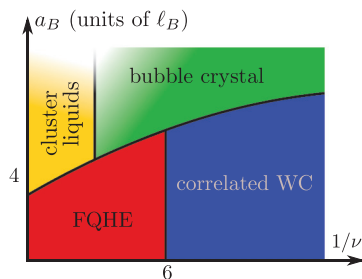


FIG. 10. (Color online) Qualitative form of the LLL phase diagram.

variety of interesting correlated phases not found in the standard FQH physics of the LLL. This has two reasons: The rapid falloff of the interaction potential with distance and the competition of two length scales, a_B and ℓ_B . A qualitative picture of the LLL phase diagram is shown in Fig. 10. In the limit of pure vdW interactions ($a_B/\ell_B \rightarrow 0$) the $\nu = 1/2, 1/4$ Laughlin states are exact ground states. Although we mainly discussed filling fractions with even values of $1/\nu$ the entire region is denoted by “FQHE” since we expect the standard bosonic FQH physics [24] to hold for all fractional fillings larger than $\nu = 1/6$. For $\nu \leq 1/6$ we find CWC ground states, while a NWC ansatz predicts crystallization only at $\nu = 1/12$. For $a_B \gtrsim \sqrt{4/\nu}\ell_B$ and $\nu \leq 1/4$ a transition to a BC is expected. Finally, for larger fillings and blockade radii the nature of the ground state is an open question, and for filling $\nu = 1/2$ we speculated on a connection to interesting cluster liquid states in particular the Hf [66].

ACKNOWLEDGMENTS

We thank J. Otterbach for helpful discussions and M. Baranov for drawing our attention to the crystal stability analysis. F.G. acknowledges financial support from the the Graduate School of Excellence MAINZ.

APPENDIX: EXACT DIAGONALIZATION

In addition to variational calculations we performed state-of-the-art ED studies. To minimize the role of finite-size effects we did all our systematic investigations in spherical geometry. We work on standard desktop computers and have excess up to the following particle numbers:

ν	1	1/2	1/4	1/6	1/8
N_{\max}	14	10	7	6	6
dim.	194 668	246 448	48 417	32 134	118 765

The dimension of the full Hilbertspace containing all angular momentum multiplets is given, since we do not explicitly exploit that $[\mathcal{H}, \vec{L}_{\text{tot}}^2] = 0$ in the numerics. In the

numerics the filling fraction ν is adjusted by changing the magnetic flux N_Φ through the surface of the sphere. For $\nu = 1/2, 1/4, \dots$ Laughlin states

$$N_\Phi = \frac{N-1}{\nu}.$$

We eliminate leading-order finite size effects by rescaling the magnetic length [67],

$$\ell_B \rightarrow \ell_B^\infty = \sqrt{\frac{N_\Phi \nu}{N}} \ell_B.$$

In simulations a_B must be chosen small enough since when the blockade area fills half a sphere, i.e., when $a_B \geq \pi \sqrt{N_\Phi/8} \ell_B$, we expect the formation of two clusters on opposite poles. We indeed found large overlaps to two-cluster trial wave functions in this case and no conclusions about the thermodynamic limit can be drawn.

In disk geometry we only performed systematic studies for small $a_B \lesssim \ell_B$ and found similar results as in spherical geometry. The accessible system sizes are the same as above, although requiring slightly more CPU time.

-
- [1] B. I. Halperin, *Phys. Rev. Lett.* **52**, 1583 (1984).
 [2] D. Arovas, J. R. Schrieffer, and F. Wilczek, *Phys. Rev. Lett.* **53**, 722 (1984).
 [3] G. Moore and N. Read, *Nucl. Phys. B* **360**, 362 (1991).
 [4] C. Nayak and F. Wilczek, *Nucl. Phys. B* **479**, 529 (1996).
 [5] P. Bonderson, V. Gurarie, and C. Nayak, *Phys. Rev. B* **83**, 075303 (2011).
 [6] A. Y. Kitaev, *Ann. Phys.* **303**, 2 (2003).
 [7] C. Nayak, S. H. Simon, A. Stern, M. Freedman, and S. Das Sarma, *Rev. Mod. Phys.* **80**, 1083 (2008).
 [8] D. J. Thouless, M. Kohmoto, M. P. Nightingale, and M. denNijs, *Phys. Rev. Lett.* **49**, 405 (1982).
 [9] N. R. Cooper, N. K. Wilkin, and J. M. F. Gunn, *Phys. Rev. Lett.* **87**, 120405 (2001).
 [10] N. R. Cooper, *Adv. Phys.* **57**, 539 (2008).
 [11] A. L. Fetter, *Rev. Mod. Phys.* **81**, 647 (2009).
 [12] G. Juzeliunas and P. Ohberg, *Phys. Rev. Lett.* **93**, 033602 (2004).
 [13] G. Juzeliunas, J. Ruseckas, P. Ohberg, and M. Fleischhauer, *Phys. Rev. A* **73**, 025602 (2006).
 [14] J. Dalibard, F. Gerbier, G. Juzeliunas, and P. Ohberg, *Rev. Mod. Phys.* **83**, 1523 (2011).
 [15] Y.-J. Lin, R. L. Compton, K. Jiménez-García, J. V. Porto, and I. B. Spielman, *Nature (London)* **462**, 628 (2009).
 [16] N. R. Cooper, *Phys. Rev. Lett.* **106**, 175301 (2011).
 [17] D. Jaksch and P. Zoller, *New J. Phys.* **5**, 56 (2003).
 [18] M. Aidelsburger, M. Atala, S. Nascimbene, S. Trotzky, Y.-A. Chen, and I. Bloch, *Phys. Rev. Lett.* **107**, 255301 (2011).
 [19] K. W. Madison, F. Chevy, W. Wohlleben, and J. Dalibard, *Phys. Rev. Lett.* **84**, 806 (2000).
 [20] J. R. Abo-Shaeer, C. Raman, J. M. Vogels, and W. Ketterle, *Science* **292**, 476 (2001).
 [21] V. Schweikhard, I. Coddington, P. Engels, V. P. Mogendorff, and E. A. Cornell, *Phys. Rev. Lett.* **92**, 040404 (2004).
 [22] N. K. Wilkin, J. M. F. Gunn, and R. A. Smith, *Phys. Rev. Lett.* **80**, 2265 (1998).
 [23] N. R. Cooper and N. K. Wilkin, *Phys. Rev. B* **60**, R16279 (1999).
 [24] N. Regnault and T. Jolicoeur, *Phys. Rev. Lett.* **91**, 030402 (2003).
 [25] M. Saffman, T. G. Walker, and K. Molmer, *Rev. Mod. Phys.* **82**, 2313 (2010).
 [26] T. Peyronel, O. Firstenberg, Q.-Y. Liang, S. Hofferberth, A. V. Gorshkov, T. Pohl, M. D. Lukin, and V. Vuletic, *Nature (London)* **488**, 57 (2012).
 [27] J. Otterbach, J. Ruseckas, R. G. Unanyan, G. Juzeliunas, and M. Fleischhauer, *Phys. Rev. Lett.* **104**, 033903 (2010).
 [28] M. Hafezi, E. A. Demler, M. D. Lukin, and J. M. Taylor, *Nat. Phys.* **7**, 907 (2011).
 [29] K. Osterloh, N. Barberan, and M. Lewenstein, *Phys. Rev. Lett.* **99**, 160403 (2007).
 [30] M. A. Baranov, K. Osterloh, and M. Lewenstein, *Phys. Rev. Lett.* **94**, 070404 (2005).
 [31] E. H. Rezayi, N. Read, and N. R. Cooper, *Phys. Rev. Lett.* **95**, 160404 (2005).
 [32] R. B. Laughlin, *Phys. Rev. Lett.* **50**, 1395 (1983).
 [33] D. Tong, S. M. Farooqi, J. Stanojevic, S. Krishnan, Y. P. Zhang, R. Cote, E. E. Eyller, and P. L. Gould, *Phys. Rev. Lett.* **93**, 063001 (2004).
 [34] K. Singer, M. Reetz-Lamour, T. Amthor, L. G. Marcassa, and M. Weidemuller, *Phys. Rev. Lett.* **93**, 163001 (2004).
 [35] T. Vogt, M. Viteau, J. Zhao, A. Chotia, D. Comparat, and P. Pillet, *Phys. Rev. Lett.* **97**, 083003 (2006).
 [36] R. Heidemann, U. Raitzsch, V. Bendkowsky, B. Butscher, R. Low, L. Santos, and T. Pfau, *Phys. Rev. Lett.* **99**, 163601 (2007).
 [37] R. Heidemann, U. Raitzsch, V. Bendkowsky, B. Butscher, R. Low, and T. Pfau, *Phys. Rev. Lett.* **100**, 033601 (2008).
 [38] M. Viteau, M. G. Bason, J. Radogostowicz, N. Malossi, D. Ciampini, O. Morsch, and E. Arimondo, *Phys. Rev. Lett.* **107**, 060402 (2011).
 [39] A. Schwarzkopf, R. E. Sapiro, and G. Raithel, *Phys. Rev. Lett.* **107**, 103001 (2011).
 [40] N. Henkel, R. Nath, and T. Pohl, *Phys. Rev. Lett.* **104**, 195302 (2010).
 [41] J. E. Johnson and S. L. Rolston, *Phys. Rev. A* **82**, 033412 (2010).
 [42] J. Otterbach, R. G. Unanyan, and M. Fleischhauer (unpublished).
 [43] M. Hafezi, A. S. Sorensen, E. Demler, and M. D. Lukin, *Phys. Rev. A* **76**, 023613 (2007).
 [44] J. K. Jain, *Composite Fermions* (Cambridge University Press, Cambridge, 2007).
 [45] N. Henkel, F. Cinti, P. Jain, G. Pupillo, and T. Pohl, *Phys. Rev. Lett.* **108**, 265301 (2012).
 [46] F. D. M. Haldane, *Phys. Rev. Lett.* **51**, 605 (1983).
 [47] V. Bretin, S. Stock, Y. Seurin, and J. Dalibard, *Phys. Rev. Lett.* **92**, 050403 (2004).

- [48] K. Singer, J. Stanojevic, M. Weidemüller, and R. Côté, *J. Phys. B* **38**, S295 (2005).
- [49] K. Maki and X. Zotos, *Phys. Rev. B* **28**, 4349 (1983).
- [50] P. K. Lam and S. M. Girvin, *Phys. Rev. B* **30**, 473 (1984).
- [51] M. A. Baranov, H. Fehrmann, and M. Lewenstein, *Phys. Rev. Lett.* **100**, 200402 (2008).
- [52] N. Metropolis, A. W. Rosenbluth, M. N. Rosenbluth, A. H. Teller, and E. Teller, *J. Chem. Phys.* **21**, 1087 (1953).
- [53] W. Pan, H. L. Stormer, D. C. Tsui, L. N. Pfeiffer, K. W. Baldwin, and K. W. West, *Phys. Rev. Lett.* **88**, 176802 (2002).
- [54] H. Fukuyama, *Solid State Commun.* **19**, 551 (1976).
- [55] Y. E. Lozovik and V. M. Farztdinov, *Solid State Commun.* **54**, 725 (1985).
- [56] S. M. Girvin, A. H. MacDonald, and P. M. Platzman, *Phys. Rev. B* **33**, 2481 (1986).
- [57] R. K. Kamilla, X. G. Wu, and J. K. Jain, *Phys. Rev. Lett.* **76**, 1332 (1996).
- [58] J. K. Jain, *Phys. Rev. Lett.* **63**, 199 (1989).
- [59] H. M. Yi and H. A. Fertig, *Phys. Rev. B* **58**, 4019 (1998).
- [60] C. C. Chang, G. S. Jeon, and J. K. Jain, *Phys. Rev. Lett.* **94**, 016809 (2005).
- [61] F. D. M. Haldane, in *The Quantum Hall Effect*, edited by R. E. Prange and S. M. Girvin (Springer, New York, 1990).
- [62] A. A. Koulakov, M. M. Fogler, and B. I. Shklovskii, *Phys. Rev. Lett.* **76**, 499 (1996).
- [63] N. R. Cooper, E. H. Rezayi, and S. H. Simon, *Phys. Rev. Lett.* **95**, 200402 (2005).
- [64] N. Read and E. Rezayi, *Phys. Rev. B* **59**, 8084 (1999).
- [65] B. A. Bernevig and F. D. M. Haldane, *Phys. Rev. Lett.* **100**, 246802 (2008).
- [66] D. Green, Ph.D. thesis, Yale University, 2001.
- [67] N. d'Ambrumenil and R. Morf, *Phys. Rev. B* **40**, 6108 (1989).
- [68] B. A. Bernevig and N. Regnault, *Phys. Rev. Lett.* **103**, 206801 (2009).
- [69] V. W. Scarola, K. Park, and J. K. Jain, *Nature (London)* **406**, 863 (2000).
- [70] M. J. Rice and Y. R. Wang, *Phys. Rev. B* **37**, 5893 (1988).